Neurobiology of Disease 70 (2014) 12–20

Contents lists available at ScienceDirect

Neurobiology of Disease

journal homepage: www.elsevier.com/locate/ynbdi

Stem cell-derived motor neurons from spinal and bulbar muscular atrophy patients

Christopher Grunseich [a,*], Kristen Zukosky [a,1], Ilona R. Kats [a,1], Laboni Ghosh [a], George G. Harmison [a], Laura C. Bott [a,b], Carlo Rinaldi [a], Ke-lian Chen [a], Guibin Chen [c], Manfred Boehm [c], Kenneth H. Fischbeck [a]

[a] Neurogenetics Branch, National Institute of Neurological Disorders and Stroke, 2A-1000 Building 35, 35 Convent Drive, NIH, Bethesda, MD 20892, USA
[b] Department of Cell and Molecular Biology, Karolinska Institute, Solnavagen 1, 17177 Solna, Sweden
[c] National Heart, Lung and Blood Institute, Bld 10-CRC Rm 5-3132, 10 Center Dr., NIH, Bethesda, MD 20892, USA

ARTICLE INFO

Article history:
Received 28 January 2014
Revised 23 April 2014
Accepted 30 May 2014
Available online 9 June 2014

Keywords:
Spinal and bulbar muscular atrophy
Induced pluripotent stem cells
Motor neuron disease
Androgen receptor

ABSTRACT

Spinal and bulbar muscular atrophy (SBMA, Kennedy's disease) is a motor neuron disease caused by polyglutamine repeat expansion in the androgen receptor. Although degeneration occurs in the spinal cord and muscle, the exact mechanism is not clear. Induced pluripotent stem cells from spinal and bulbar muscular atrophy patients provide a useful model for understanding the disease mechanism and designing effective therapy. Stem cells were generated from six patients and compared to control lines from three healthy individuals. Motor neurons from four patients were differentiated from stem cells and characterized to understand disease-relevant phenotypes. Stem cells created from patient fibroblasts express less androgen receptor than control cells, but show androgen-dependent stabilization and nuclear translocation. The expanded repeat in several stem cell clones was unstable, with either expansion or contraction. Patient stem cell clones produced a similar number of motor neurons compared to controls, with or without androgen treatment. The stem cell-derived motor neurons had immunoreactivity for HB9, Isl1, ChAT, and SMI-32, and those with the largest repeat expansions were found to have increased acetylated α-tubulin and reduced HDAC6. Reduced HDAC6 was also found in motor neuron cultures from two other patients with shorter repeats. Evaluation of stably transfected mouse cells and SBMA spinal cord showed similar changes in acetylated α-tubulin and HDAC6. Perinuclear lysosomal enrichment, an HDAC6 dependent process, was disrupted in motor neurons from two patients with the longest repeats. SBMA stem cells present new insights into the disease, and the observations of reduced androgen receptor levels, repeat instability, and reduced HDAC6 provide avenues for further investigation of the disease mechanism and development of effective therapy.

Published by Elsevier Inc.

Introduction

Our understanding of the pathogenesis of motor neuron disease has been limited by the paucity of model systems that can recapitulate disease features as they occur in vivo. SBMA is caused by a CAG repeat expansion in the androgen receptor (AR) gene on the X chromosome (La Spada et al., 1991), which results in polyglutamine expansion and an androgen-dependent toxic gain of function in the mutant protein. SBMA patients have repeat lengths between 38 and 62 CAGs; whereas normal individuals have between 5 and 36 CAGs (Atsuta et al., 2006; Rhodes et al., 2009). The length of the CAG repeat correlates inversely with the age of disease onset, with longer repeats associated with earlier onset. The affected males have a slowly progressive deficit with weakness of the limb and bulbar muscles due to lower motor neuron and muscle degeneration. There is currently no treatment available to affect the progression of this disease, and although cellular processes such as transcriptional regulation (Nedelsky et al., 2010), mitochondrial function (Ranganathan et al., 2009), and axonal transport (Katsuno et al., 2006) have been implicated, the precise mechanism underlying the pathology is not clear.

The induced pluripotent stem cell (iPSC) system provides a unique opportunity in which stem cells can be generated from adult patients and then differentiated into disease-relevant progeny such as neurons, glia, and muscle. This technology has been used to generate and differentiate iPSCs from patients with motor neuron diseases such as ALS

Abbreviations: AR, androgen receptor; DHT, dihydrotestosterone; EtOH, ethanol; iPSC, induced pluripotent stem cell; SBMA, spinal and bulbar muscular atrophy.

* Corresponding author.
E-mail addresses: christopher.grunseich@nih.gov (C. Grunseich), kristen.perkins@nih.gov (K. Zukosky), Ilona.kats@nih.gov (I.R. Kats), labonighosh@gmail.com (L. Ghosh), george.harmison@nih.gov (G.G. Harmison), laura.bott@nih.gov (L.C. Bott), carlo.rinaldi@nih.gov (C. Rinaldi), chenk@ninds.nih.gov (K. Chen), guibin.chen@nih.gov (G. Chen), manfred.boehm@nih.gov (M. Boehm), kf@ninds.nih.gov (K.H. Fischbeck).

Available online on ScienceDirect (www.sciencedirect.com).

[1] These authors contributed equally to this work.

http://dx.doi.org/10.1016/j.nbd.2014.05.038
0969-9961/Published by Elsevier Inc.

(Dimos et al., 2008). A phenotype has been described in motor neuron cells differentiated from spinal muscular atrophy (SMA) iPS cells (Ebert et al., 2009). An assay for screening small molecules in such a system may also be expected to yield more disease-relevant results, since it is human patient-derived. Motor neuron-like cells derived from ALS patients with mutations in TDP-43 have been used to screen candidate chemical compounds (Egawa et al., 2012). These systems offer the potential advantage of reproducing the cellular and molecular features of the disease, with physiological levels of mutant protein expression. Additional insights into the disease mechanism may provide new targets for therapeutic development.

In this study we generated lines from six SBMA patients, and performed a detailed evaluation of lines from four different patients and three controls. The SBMA iPSCs retain the CAG repeat expansion present in the parental fibroblasts, and in some cases variation from the parental CAG repeat length was observed. We found that the AR is expressed in the undifferentiated iPSCs, and able to translocate to the nucleus in response to ligand treatment. The iPSC lines were differentiated into motor neurons, and further characterization of these cells was done. Motor neuron derivatives from the SBMA iPSCs were found to have a reduction in HDAC6. The iPSCs described here are valuable tools for understanding the disease process, and they provide a system for evaluating candidate treatments.

Materials and methods

iPSC generation

Lentiviral vectors containing the polycistronic transcripts Oct4, Klf4, Sox2, and c-Myc (Sommer et al., 2009) were purchased from Millipore (Billerica, MA) and Stemgent (Cambridge, MA). Human fibroblasts were seeded at 2.5×10^4 cells/well on a 6-well plate. For the next two days the fibroblasts were transduced with virus and plated onto a feeder layer of mitomycin-c treated MEF cells at day 6. Colonies with hESC morphology were mechanically dissociated after three weeks. Sendai virus was purchased from Invitrogen (Carlsbad, CA) and used according to the manufacturer's instructions. Episomal vectors were purchased from Addgene (Cambridge, MA) and cotransfected into fibroblasts using the U-20 Amaxa nucleofection program (Walkersville, MD). After expansion, the iPSCs were maintained in mTESR media (Stem Cell Technologies, Vancouver, Canada).

CAG repeat sizing

Polymerase chain reaction (PCR) was performed using Taq polymerase-containing master mix (FastStart PCR Master; Roche, Basel, Switzerland), with 20 nM forward and reverse primers (5′-TCCAGAATCTGTTCCAGAGCGTGC-3′ and 5′-GCTGTGAAGGTTGCTG TTCCTCAT-3′, respectively). PCR products were analyzed on a 20% Tris–borate–EDTA gel (Invitrogen). The Big Dye cycling protocol (Invitrogen) was performed using a two step method without the annealing step (96 °C 10 s, 60 °C 4 min).

Motor neuron differentiation

Differentiation was performed as previously described (Amoroso et al., 2013). Briefly, iPSCs were grown to 80% confluency, then digested with collagenase IV (Invitrogen) for 8 min. Cells were scraped off of the dish, and after settling the supernatant was aspirated, and cells were re-plated into low adherence dishes (Corning, Corning, NY) in KSR (Invitrogen) based media with 20 ng/ml FGF (R + D Systems, Minneapolis, MN), 20 μM ROCK-I (Tocris, Bristol, UK), 10 μM SB431542 (Tocris), and 0.2 μM LDN193189 (Stemgent). Embryoid bodies (EBs) were transitioned to a KSR free medium after 3 days. Retinoic acid was added to the media after 5 days to direct the cells towards a rostral spinal cord phenotype, with additional patterning using 1 μM smoothened agonist (Calbiochem, Billerica, MA) and 0.5 μM purmorphamine (Stemgent) after 7 days to ventralize the differentiating population. After 14–16 days in suspension, the EBs were dissociated and plated on dishes coated with polyornithine or poly-D-lysine and laminin for an additional 7–14 days. Neuronal cultures were maintained in neurobasal media (Invitrogen) with 25 μM glutamate (Sigma, St. Louis, MO), 0.4 μg/ml ascorbic acid (Sigma), 10 ng/ml GDNF (Sigma), 10 ng/ml CNTF (Sigma), 1 μg/ml laminin (BD Bioscience, Franklin Lakes, NJ). B-27, N2, non-essential amino acids, and pen/strep/glutamine were all from Invitrogen. Two days after plating 10 nM dihydrotestosterone (DHT) was added, and the cultures were maintained for an additional 7–14 days.

Immunoblotting

Cell pellets were lysed with RIPA buffer [150 mM NaCL, 1% NP40, 0.5% sodium deoxycholate, 0.1% SDS, 50 mM Tris pH 8.0 and Protease inhibitor cocktail (Roche)] and allowed to stand on ice for 20 min before being centrifuged at 4 °C at 20,000 *g* for 20 min. Supernatant was collected and protein levels were measured using a Bio-Rad (Hercules, CA) protein assay. Membranes were blocked with a 5% milk solution and incubated in milk with primary antibody overnight. The antibodies used were AR H280 and AR N20 (Santa Cruz Biotech., Santa Cruz, CA), GAPDH (EnCor Biotechnology, Gainesville, FL), ChAT (Millipore), MNX1/HLXB9 (Novus, Littleton, CO), HDAC6 D2E5 and LAMP1 (Cell Signaling, Danvers, MA). Stacking gel analysis for aggregation analysis was performed on supernatant samples prepared after centrifugation at 4 °C for 10 min at 425 *g*. PNGaseF was purchased from New England Biolabs (Ipswich, MA), and treatments were performed for 3 h using the manufacturer's guidelines.

Immunohistochemistry

After fixation with 4% paraformaldehyde, slides were placed in blocking solution (10% normal goat serum, 0.3% Triton X-100, in phosphate-buffered saline (PBS)) for 45 min at room temperature. Primary antibody staining was done at 4 °C overnight in PBS with 5% normal goat serum and 0.1% Triton X-100 using Oct-3/4 (Santa Cruz), GSK-3β Phospho Ser9 (Cell Signaling), AR H280 and N20 (Santa Cruz), Tra-1-60, 1C2, and Chat (Millipore), Isl1 and HB9 (DSHB, Iowa City, IA), SMI 32 and β-tubulin (Covance, Princeton, NJ), HDAC6 and LAMP1 (Cell Signaling), and acetylated tubulin and neurofilament (Sigma). Slides were then washed three times with PBST (0.1% Triton X-100 in PBS), incubated with secondary antibody (Invitrogen, 1:500) for 1 h at room temperature in the dark, and then washed three times before drying and adding vectashield/DAPI stain (Vector Lab, Burlingame, CA). For AR staining in motor neurons, slides were treated with 100 mM glycine after fixation, and blocked in PBS with 3% bovine serum albumin (BSA). Antibody staining was performed in PBS with 3% BSA and 0.1% Tween with 0.1% Tween/PBS used for all washes. Coverslips were mounted with permamount (Thermo, Waltham, MA).

Results

Derivation and characterization of iPSC from SBMA patients and controls

IPSC lines were derived using forearm fibroblasts from six SBMA patients (SB1, 3, 6, 15, 17, and 18) and three healthy control adults (NC4, 7, and 15) (Table 1). All iPSC lines chosen for evaluation had expression of pluripotency markers by immunostaining and quantitative PCR (Fig. S1). Karyotype analysis was normal in 12 clones tested, from which 5 patient (Fig. 1, asterisks) and 3 control lines were chosen for further analysis. Down-regulation of Oct4 was observed in the motor neuron derivatives from the iPSC, showing sufficient down regulation of the polycistronic vector. Teratoma analysis was done for the SB6MP2 clone.

Table 1
iPS lines used.

iPS line	NC4	NC7	NC15	SB1	SB3	SB6	SB15	SB17	SB18
Age of onset	N/A	N/A	N/A	39	53	32	34	25	18
Age	31	23	51	59	68	37	49	43	29
Sex	Male	Male	Female	Male	Male	Male	Male	Male	Male
Reprogramming method	Millipore *Lentivirus*	Millipore *Lentivirus*	Millipore *Lentivirus*	Stemgent *Lentivirus* (all)	Millipore *Lentivirus* (all)	Millipore *Lentivirus* (clones 1 + 2). Episomal (clone #3)	Sendai virus (all)	Millipore *Lentivirus* (all)	Millipore *Lentivirus* (all)

The CAG repeat of the AR gene was analyzed with PCR amplification and Sanger sequencing. Several of the iPSC clones showed differences in the repeat size in comparison to the parental fibroblasts (Fig. 1). This difference was most striking for the SB6 iPSC clones, which increased by six CAGs from 56 CAGs in the fibroblasts to 62 CAGs in the three iPSC clones evaluated. iPSCs with shorter CAG lengths than the parental fibroblast were found with Sendai virus reprogramming in the SB15 lines, with two of the lines having four fewer CAGs. With subsequent passaging the repeat region was stable in the three lines evaluated. CAG length remained the same between the parental fibroblasts and iPSCs in all three control lines evaluated (data not shown).

Androgen receptor expression in iPSCs

To determine whether SBMA iPSCs have the capacity to develop phenotypic abnormalities, we first evaluated undifferentiated cells for AR expression and localization. Expression and nuclear translocation of the AR in response to ligand (DHT) treatment were observed in the 3 control and 4 SBMA iPSC lines evaluated (Fig. 2A, the SBMA lines used are labeled by an asterisk in Fig. 1). Although the mutant AR has been observed to form inclusions in patient tissue and other cellular models of SBMA, inclusions were not detected in the SBMA iPSCs. We assayed for inclusions by immunostaining iPSCs and their derivatives for the androgen receptor and polyglutamine repeat motif (1C2 antibody), as well as western blotting of extracts including the stacking portion of an acrylamide gel (Fig. S4).

We next compared the AR expression levels in the iPSCs to fibroblasts. Human control and SBMA fibroblasts had a similar response to DHT as found in iPSCs (Fig. 2B). SBMA iPSC lines had significantly lower AR levels ($p < 0.001$) than the control lines, and this difference was also present after DHT treatment for 48 h ($p < 0.001$). AR mRNA expression in SBMA and control cells did not show a difference with either vehicle or DHT. These observations suggest that the AR behaves similarly in iPSCs as in other cell systems, and that the level of AR protein in SBMA iPSCs is reduced compared to control lines.

Motor neuron differentiation and characterization

Since motor neuron degeneration is one of the characteristic features in SBMA, we sought to differentiate the iPSCs into a motor neuron lineage using an established protocol (Amoroso et al., 2013) (Fig. 3A). Within one day of dissociation, control and SBMA cells extended processes. Two days after plating, fresh neuronal culture media was added with either vehicle or DHT, and the cells were then cultured for 10 days. Immunostaining for the motor neuron markers HB9 and Isl1 showed approximately 20–30% positive cells. There was no significant difference in the number of motor neurons generated between control and patient iPSCs with either vehicle or DHT (Fig. 3B). However, cultures from the SB18 patient line had approximately 14% motor neurons compared to an average of 24% for the other SBMA lines. The processes in both sets of cultures had positive staining for β-tubulin and SMI-32, markers expressed in primary motor neurons and corticospinal tract neurons (Fig. S2). Immunostaining showed that the AR is expressed in the motor neurons, although the relative amount of expression in some motor neurons was less than in other non-motor neuron cells within the same culture, as shown by the arrows in Fig. 3C. Nuclear AR staining was also seen in the absence of DHT (Fig. 3C), although increased levels were observed after DHT treatment in both control and SBMA cultures (Fig. 4D).

We found increased staining for acetylated α-tubulin in several of the SBMA iPSC clones (Fig. 4A). Although this was occasionally seen in the SB3 and SB1 lines, it was most consistent in the SB6MP2 and SB6MP3 clones, which both contain 62 CAGs. Staining for other markers of the processes, including neurofilament, was similar between SB6 and control lines. Motor neuron derivatives from the SB18 line with 68 CAGs were also found to have increased acetylated tubulin (Fig. S3). There was no appreciable difference in the extent of acetylation with DHT treatment, and all immunostaining images of cells under these conditions are shown with vehicle only.

As HDAC6 is one of the major deacetylating enzymes for α-tubulin, we sought to evaluate the levels of HDAC6 in our control and SBMA motor neuron cultures. Immunostaining for HDAC6 showed cytoplasmic localization, and the motor neurons had higher levels than other cells in the culture (Figs. 4C, S3). HDAC6 levels in several SBMA lines were reduced compared to controls, $p < 0.001$. HDAC6 levels were adjusted based on the total level of HB9 and Isl1 staining. Western blot analysis across the control and SBMA iPSCs also showed a reduction in HDAC6 levels, with comparable amounts of ChAT and HB9 detected. As GSK-3β inhibition is known to decrease HDAC6 levels, we evaluated the degree of GSK-3β activation by immunostaining for the inactive form of GSK-3β (Ser9) and found comparable levels in SBMA and control motor neurons.

We next sought to determine whether tubulin and HDAC6 are similarly altered in another cell model system of SBMA and patient tissue. We assessed murine motor neuron-neuroblastoma (MN1) cells stably transfected with human AR containing either 24 or 65 CAGs (Brooks et al., 1997). After 48 h of DHT treatment, the cells were evaluated for HDAC6 and acetylated α-tubulin by immunostaining and western blot (Fig. 5A). The MN1 cells with the unexpanded CAG repeat have abundant cytoplasmic HDAC6 and reduced staining for acetylated tubulin, whereas the MN1 clone with expanded 65Q AR had reduced HDAC6 levels and increased levels of acetylated tubulin ($p = 0.03$) after DHT treatment. A similar pattern was also observed in the ventral horn of the spinal cord of a control subject and a patient showing that the patient tissue had increased staining for acetylated α-tubulin and reduced motor neuron staining for HDAC6 (Fig. 5B).

Since microtubule-mediated transport of intracellular organelles can be disrupted by HDAC6 deficiency (Iwata et al., 2005), we analyzed the location of lysosomes in the motor neuron derivatives. Staining for the lysosomal marker LAMP1 in the control motor neurons showed enrichment of staining around the microtubule organizing center (Fig. 6A). LAMP1 staining in the motor neuron cultures from the SB6 and SB18 SBMA iPSC lines with the largest CAG repeats showed more diffuse staining around the nucleus. Western blot analysis of the motor neuron extracts for LAMP1 showed increased molecular weights in the SB6 and SB18 patient lines with or without DHT (Fig. 6B). These changes in LAMP1 molecular weight were not detected in the undifferentiated DHT-treated iPSCs (Fig. 6C). Since LAMP1 is known to be heavily glycosylated, we removed the N-glycans by PNGaseF treatment and analyzed the samples for LAMP1. Western blot showed bands of similar molecular weight in all samples with the predominant bands at 40 and 42 kDa (Fig. 6D).

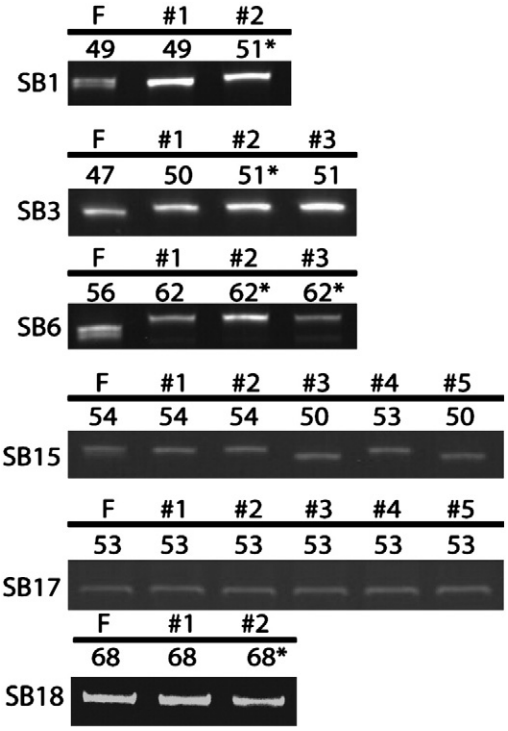

Fig. 1. Expansion and contraction of CAG polyglutamine repeat during the induction of pluripotency. Polyacrylamide gels show changes in CAG repeat length in different colonies from multiple iPSC lines. F refers to the fibroblast sample from which the iPSCs were derived. The asterisk notation refers to those patient lines that were chosen for further analysis of AR expression and differentiation.

Discussion

We generated iPSCs from SBMA patients in order to characterize phenotypic features that can be used to elucidate the disease mechanism. Although the AR is expressed in many tissues, it is not clear why certain cells are vulnerable in the disease, such as anterior horn cells, dorsal root ganglion cells, and skeletal muscle (Iwata et al., 2005; Kennedy et al., 1968). At present there is no treatment to slow the disease progression, and better understanding of the pathogenesis may help in identifying therapeutic targets.

Patient-derived iPSCs grow and differentiate like human embryonic stem cells. Although SBMA iPSC clones generally have CAG repeat lengths similar to the parental fibroblasts, we have identified clones with CAG repeat lengths that are longer or shorter. The differences in iPSC repeat length could be due to repeat instability during the cloning or to repeat length mosaicism in the parental fibroblast population. Repeat instability occurs between generations in patients, more frequently during transmission of the mutant allele from father to daughter (Zhang et al., 1994). It is possible that chromatin remodeling during reprogramming recapitulates processes similar to those that take place during meiosis and gametogenesis (Xu et al., 2011). Somatic mosaicism has also been observed in polyglutamine diseases (Tanaka et al., 1999), and it is also conceivable that mosaicism within the fibroblast population results in clonal expansion of different CAG repeat sizes represented in the fibroblast pool. This may explain some of the smaller differences in repeat size, but it is less likely to be present in the clones which more consistently have substantial variation from the parental fibroblasts, such as the clones from the SB6 fibroblasts. In a previous study of SBMA iPSCs (Nihei et al., 2013), the CAG repeat length was unchanged in two clones from one patient and, as with our lines, stable with long term passaging.

Our findings show that the AR is expressed in iPSCs and undergoes nuclear translocation as in other cells expressing AR. The level of AR is increased with ligand (DHT) treatment at the protein level only, suggesting that the increased level is a result of protein stabilization, as has been shown in other cell lines (Furutani et al., 2002). The AR appears to be expressed at equal or higher levels in all of the iPSCs evaluated compared to human fibroblasts, as assessed by both quantitative PCR and western blotting. This finding is in contrast to the previous iPSC study which showed that AR protein levels in iPSCs were negligible, and reduced compared to fibroblasts (Nihei et al., 2013). The reason for this discrepancy is not clear, however, it may be due in part to differences in cell culture technique.

The finding of reduced AR protein levels in the SBMA iPSCs was reproduced in lines from four patients compared to three controls. This difference was detected with and without DHT, and appeared to occur at the protein level, since AR mRNA levels were roughly equal. This difference was detected when the cells were cultured in two different types of media, mTeSR and E8. It is possible that selective pressure led to the expansion and growth of SBMA iPSC colonies that had reduced AR levels. If selective pressure occurs, then this may reflect toxicity of the mutant AR in the SBMA iPSCs, perhaps during reprogramming. It is possible that the SBMA iPSCs are similar to controls in other ways because of compensatory down-regulation in AR levels. We have not detected any abnormality in the survival of the SBMA iPSCs after maintaining the cells with DHT for five passages. However, it is possible that treatment with additional factors to stabilize the mutant AR would induce overt toxicity in the undifferentiated SBMA iPSCs. It does not appear that the AR protein reduction is dependent on the length of the CAG repeat, as no such association was observed. The reduction in mutant AR levels in iPSCs may also recapitulate the androgen insensitivity in SBMA patients, who often have features of gynecomastia, oligospermia, and reduced androgenic alopecia (Rhodes et al., 2009; Sinclair et al., 2007). The CAG repeat length is predictive of the onset of disease in SBMA patients, but has not been shown to be related to the severity of androgen insensitivity.

Our iPSC model system provides the opportunity to evaluate the relative contribution of specific cell types to the disease pathogenesis. An evaluation of the potential for motor neuron differentiation shows that SBMA iPSCs differentiate into HB9 and Isl1 positive motor neurons with an efficiency similar to controls. The SB18 line with a 68 CAG repeat was observed to have a decrease in motor neuron generation, which was not DHT dependent. This finding may be limited to the SB18 line because of its relatively large CAG repeat size. It is possible that the nuclear AR detected in the vehicle treated neurons (Fig. 3C) may be masking any differences with DHT treatment. Furthermore, there is also no reduction in the number of cultured motor neurons maintained in DHT for 10 days after dissociation in the other patient cultures. This finding is consistent with analysis of motor neuron counts from the spinal cord of SBMA model mice which do not show a significant reduction of motor neuron numbers (Katsuno et al., 2002; Palazzolo et al., 2009). The finding that control and SBMA motor neuron cultures have well developed processes that stain for SMI-32, β-tubulin, and neurofilament suggests that the differentiation potential of the SBMA motor neuron cells is intact. Our differentiated motor neurons express AR, although the nuclear signal is not as strong as in other non-motor neuron cells within the culture. It is interesting that motor neurons in general also have higher levels of phosphorylated GSK-3β, as GSK-3β inhibition has been shown to increase nuclear export of the AR in prostate cancer cell models (Schutz et al., 2011).

The motor neurons from patient SB6 with 62 CAGs and patient SB18 with 68 CAGs had increased acetylated α-tubulin compared to controls. The increased acetylation of α-tubulin may be a consequence of reduced HDAC6 activity. HDAC6 levels were decreased in the SBMA motor neuron cells from several patient lines, including the iPSC lines with 51 CAGs. Although a reduction in HDAC6 protein was detected in motor neuron cultures from patient lines containing 51 CAGs, the changes in acetylated α-tubulin were seen only in the cultures with 62 and 68 CAGs. It is possible that other changes in the 62 and 68 CAG lines allowed this alteration to occur. The importance of this HDAC6

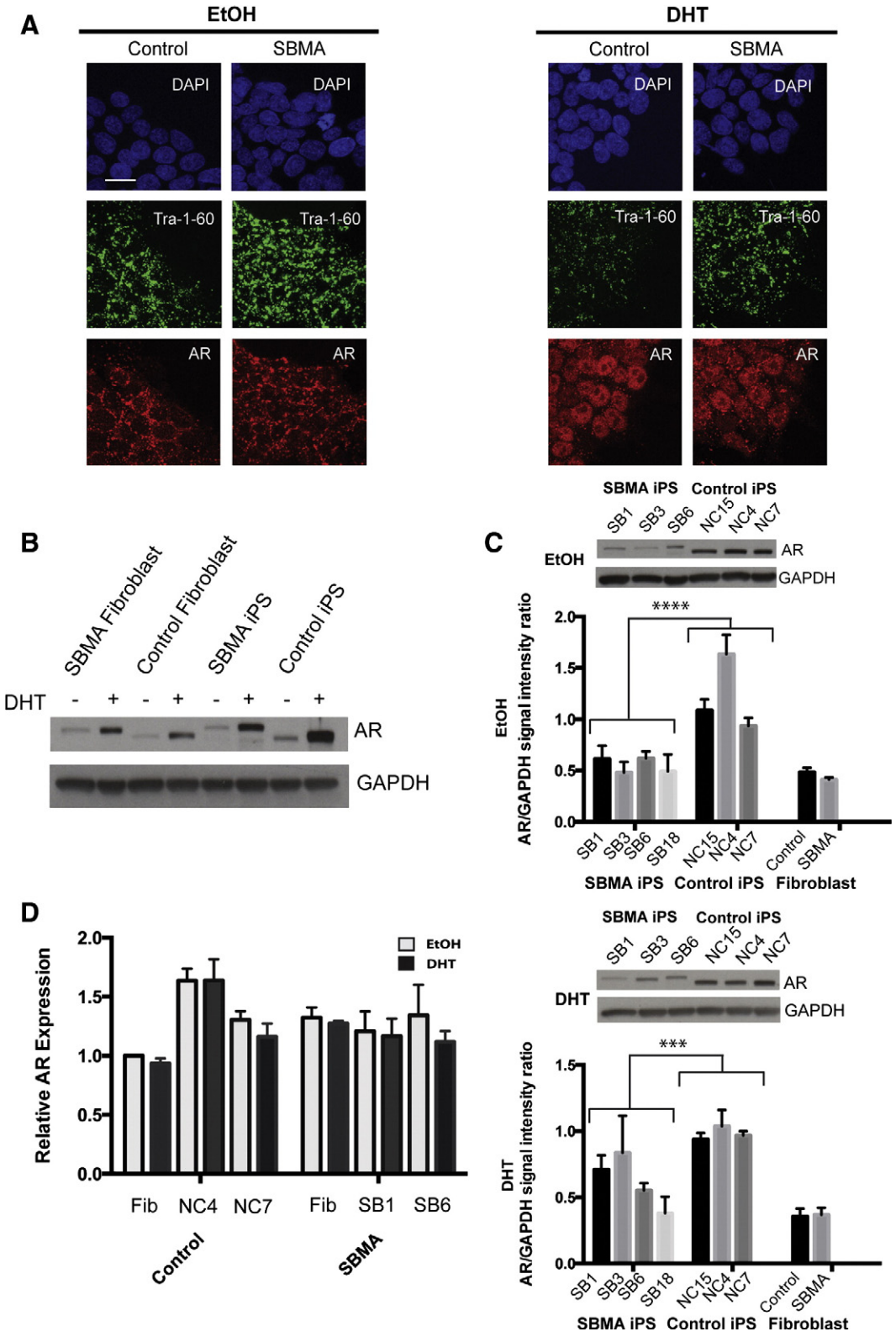

Fig. 2. Androgen receptor (AR) expression in iPSCs derived from patients with spinal and bulbar muscular atrophy (SBMA). (A) Immunofluorescence images show that iPSCs treated with dihydrotestosterone (DHT) have increased AR localization in the nucleus compared to iPSCs treated with the ethanol vehicle alone (EtOH). DAPI (blue), Tra 1-60 (green) and AR (red). Scale bar = 10 μM. (B) Western blot comparing AR in SBMA and control samples treated with EtOH or DHT shows increased AR with DHT. (C) AR levels are decreased in SBMA lines compared to controls, either with EtOH vehicle alone or with DHT. Insets show representative western blots of AR in EtOH-and DHT-treated iPSCs. n ≥ 3 (D) AR mRNA levels in SBMA and control cells are similar with or without DHT when measured by quantitative RT-qPCR standardized to GUSB. Error bars represent standard error of the mean n = 3; 2-way ANOVA, ***p = 0.001, ****p < 0.001.

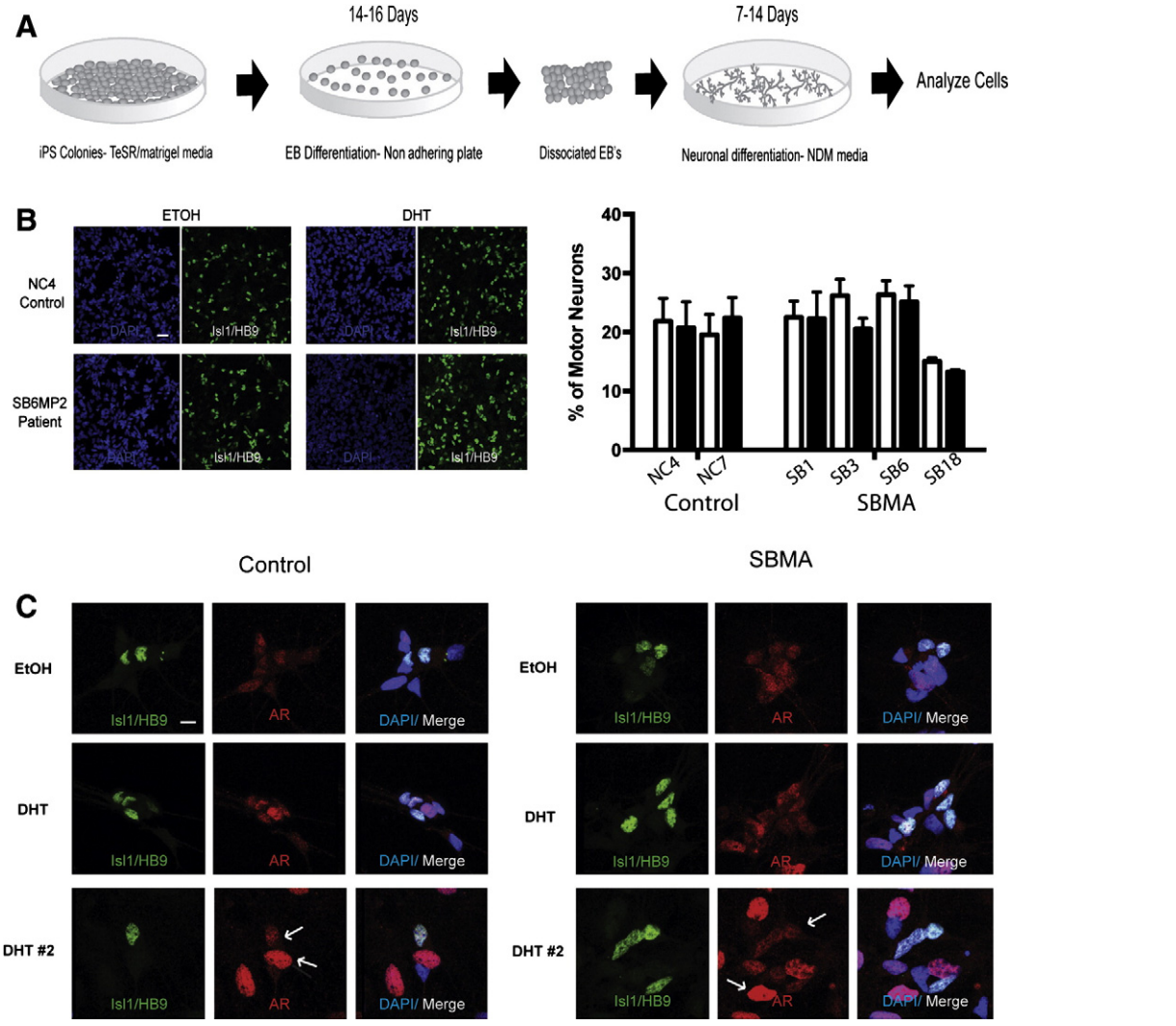

Fig. 3. Motor neuron differentiation from iPSCs. (A) Protocol timeline for differentiation of iPSCs, EB = embryoid body, NDM = neuronal differentiation media. (B) Representative immunoflourescent image showing equivalent motor neuron numbers in EtOH- and DHT-treated control and SBMA motor neurons stained for Isl1/HB9 (green) and DAPI (blue). There is no measurable difference in the percentage of Isl1/HB9 positive motor neurons compared to total cells among the different control and SBMA lines. Scale bar = 40 μM. (C) AR staining (red) in SBMA and control motor neurons (Isl1/HB9) showing increased AR intensity with DHT treatment (two sets of images with DHT treatment are shown), DAPI (blue). Scale bar = 10 μM.

down-regulation in the pathogenesis of SBMA is not clear. HDAC6 has catalytic domains responsible for deacetylating various targets, including α-tubulin (Hubbert et al., 2002), HSP-90 (Kovacs et al., 2005), cortactin (Zhang et al., 2007), and Ku-70 (Subramandian et al., 2011) as well as a ubiquitin C-terminus hydrolase-like zinc finger domain, which can bind to polyubiquitinated midfolded proteins and dynein motors, allowing for their proper autophagic clearance to aggresomes (Kawaguchi et al., 2003). HDAC6 deficiency has also been reported to disrupt the organization of the axon initial segment which is important in preferential concentration of ankyrinG and sodium channels in neurons (Tapia et al., 2010). In addition, HDAC6 may increase AR stability by deacetylating its chaperone protein HSP-90 (Ai et al., 2009).

HDAC6 may also function in the transport of lysosomes to the microtubule organizing center (MOC), as HDAC6 knockdown produces dispersion of lysosomes from the MOC. In a study by Iwata et al. (2005), shRNA mediated HDAC6 knockdown in HeLa cells resulted in dispersion of lysosomal LAMP2 staining around the nucleus. The lysosomal staining pattern detected in this study was similar to what we observed in SBMA iPSC motor neurons with reduced HDAC6 staining. We also found that LAMP1, a marker of lysosomes, is hyperglycosylated in the iPSC-derived SBMA motor neurons. A similar finding was reported in myoblast cultures from patients with Paget's disease and frontotemporal dementia (IBMPFD) (Vesa et al., 2009). In that study, myoblasts with mutations in the valosin containing protein (VCP) gene were found to have differential glycosylation of LAMP1 and LAMP2 and enlarged autophagosomes. iPSC-derived SBMA motor neurons have alterations in lysosomal localization and post-translational modification, which may be a consequence of a disruption in HDAC6 mediated microtubule transport.

HDAC6 has previously been implicated in SBMA, as it was found to enhance autophagy to compensate for impairment of the ubiquitin–proteasome system in a *Drosophila* model (Pandey et al., 2007). In this model, ectopic expression of either *Drosophila* or human HDAC6 rescued the degenerative phenotype caused by polyglutamine expanded AR. Changes in protein acetylation have also been reported in a PC12 model of SBMA in which polyglutamine expanded AR was hyperacetylated compared to normal AR (Montie et al., 2011). Expression of the deacetylating enzyme SIRT1 protected mouse motor neurons expressing the mutant AR, suggesting that AR acetylation may be a therapeutic target in SBMA.

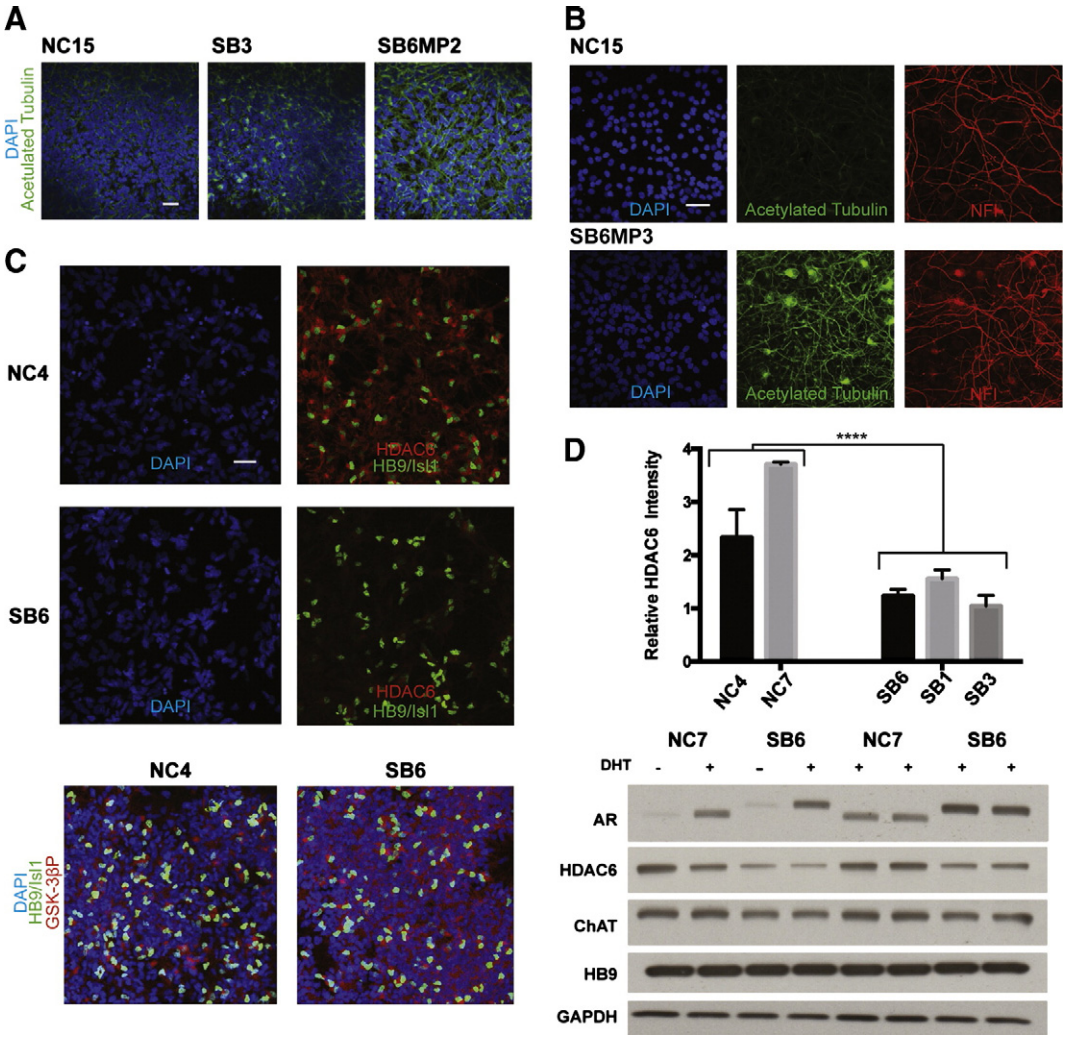

Fig. 4. α-Tubulin acetylation is increased in SBMA iPSC derived motor neurons. (A) Immunofluorescent images showing acetylated tubulin (green) and DAPI (blue) in differentiated motor neurons from a control (NC15) line and lines from two SBMA patients (SB3 and SB6MP2). The line with high repeat length, SB6MP2 (62 CAGs) shows increased acetylation. (B) Images stained for DAPI (blue), and for acetylated tubulin (green), and neurofilament (red) in control and patient-derived motor neurons from a separate clone (SB6MP3) with 62 CAGs also shows increased tubulin acetylation. (C) Decreased HDAC6 in an SBMA patient line (SB6), as shown by staining with DAPI (blue), HDAC6 (red) and HB9/Isl1 (green). Phosphorylated GSK-3β (red) remains unchanged. (D) Relative HDAC6 levels in two control and three SBMA lines, with a representative western blot (n = 3) showing decreased HDAC6 in differentiated patient and control cells with staining for ChAT and HB9 shown for comparison. The difference between patient and control lines for quantification of HDAC6 immunofluorescence relative to Isl1/HB9 is significant; n = 3, student's t-test, ****$p < 0.001$. All scale bars = 40 μM.

Conclusions

Our study demonstrates several findings in the SBMA iPSCs that warrant additional investigation. The finding that CAG repeat length is unstable in specific iPSC lines allows additional study of factors that may be involved in the expansion or contraction of the repeat. It is possible that genetic factors in some lines make them more susceptible to instability, or that factors intrinsic to the reprogramming strategy modify the instability. SBMA iPSCs appear to have motor neuron differentiation capacity equivalent to controls, and although no changes in cell survival could be appreciated it is possible that treatment with additional stressors would induce a selective vulnerability. Although increased acetylated α-tubulin was observed predominantly in cells from two patients with particularly long repeats, the HDAC6 decrease was also observed in motor neurons cultured from several others. Decreased HDAC6 and increased acetylated α-tubulin levels were also seen in an MN1 cell model of SBMA, and in the spinal cord of an SBMA patient. Since HDAC6 has been shown to be important for trafficking misfolded protein to the aggresome, a deficiency in HDAC6 may produce a reduction in autophagic flux, with changes in mitochondrial activity, protein trafficking, and lysosomal function. Changes in lysosomal localization were observed in the SBMA motor neurons, and the lysosomal marker LAMP1 was found to have increased glycosylation. The significance of this glycosylation is not clear at this time, but it appears to indicate abnormal function of the lysosomal compartment. Further studies may help to determine how HDAC6 levels are reduced in SBMA and to characterize the consequence of these changes in the disease mechanism.

Conflict of interest

None declared.

Funding

This work was supported by intramural funding from the National Center for Regenerative Medicine and the National Institute of Neurological Disorders and Stroke, NIH.

Supplementary data to this article can be found online at http://dx.doi.org/10.1016/j.nbd.2014.05.038.

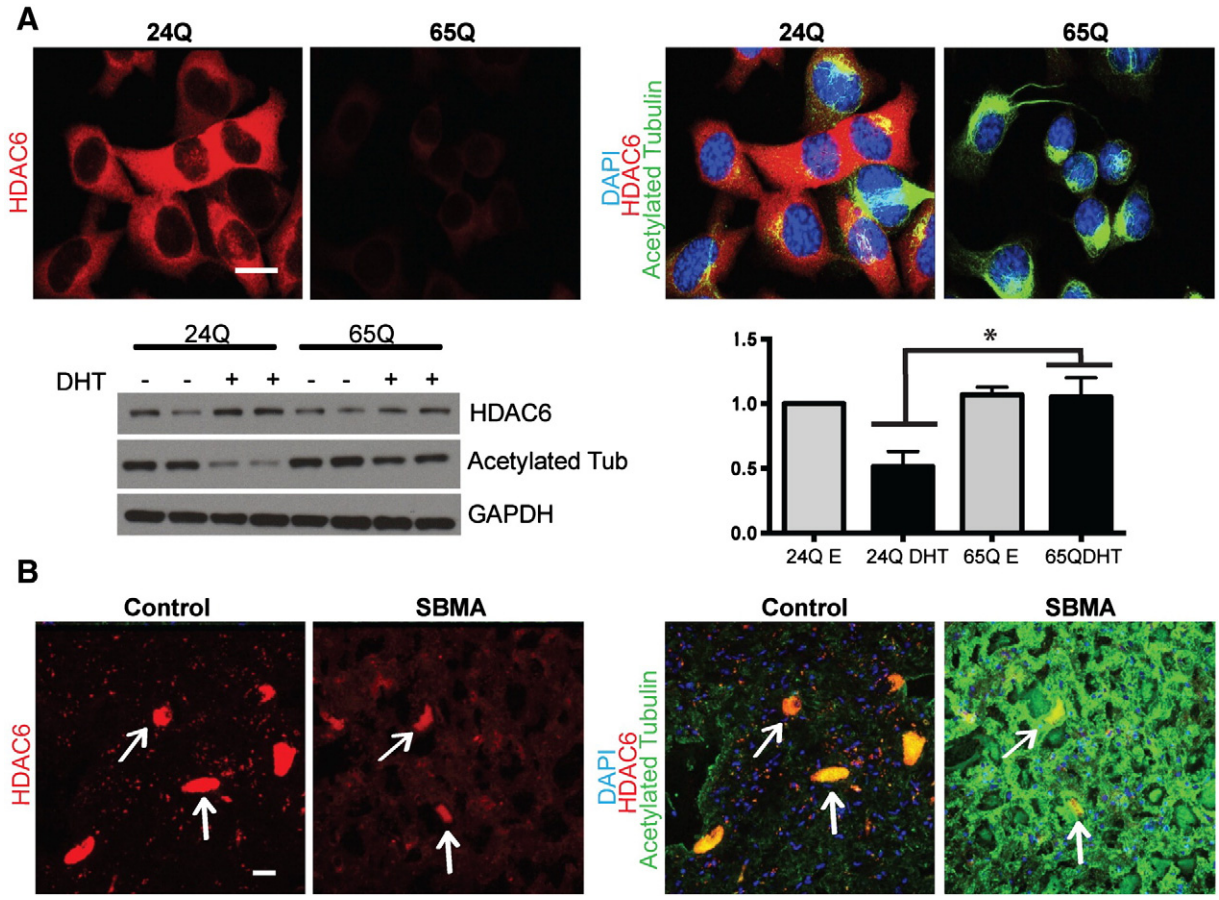

Fig. 5. Acetylated tubulin and HDAC6 staining in MN1 cells and human spinal cord. (A) Murine MN1 cells expressing either 24Q or 65Q full length human AR treated with DHT for 48 h and then stained for DAPI (blue), acetylated tubulin (green), and HDAC6 (red). Western blot analysis on 24Q and 65Q cells treated with EtOH (vehicle) or DHT for 48 h. There is decreased HDAC6 and increased acetylated tubulin ($n = 4$, $p = 0.03$) in the DHT treated 65Q AR cells compared to treated AR24Q cells. (B) Human spinal cord from a control and an SBMA patient stained for DAPI (blue), HDAC6 (red), and acetylated tubulin (green), with motor neurons (indicated by arrows) showing decreased levels of diffuse HDAC6 and increased acetylated tubulin in the SBMA patient. Scale bars = 20 μM.

Acknowledgments

We thank Dr. Nicholas Maragakis (Johns Hopkins University) for providing the control spinal cord tissue and Dr. Hynek Wicterle (Columbia University) for his advice and assistance with the motor neuron differentiation protocol.

References

Ai, J., et al., 2009. HDAC6 regulates androgen receptor hypersensitivity and nuclear localization via modulating Hsp90 acetylation in castration-resistant prostate cancer. Mol. Endocrinol. 23, 1963–1972.
Amoroso, M.W., et al., 2013. Accelerated high-yield generation of limb-innervating motor neurons from human stem cells. J. Neurosci. 33, 574–586.
Atsuta, N., et al., 2006. Natural history of spinal and bulbar muscular atrophy (SBMA): a study of 223 Japanese patients. Brain 129, 1446–1455.
Brooks, B.P., et al., 1997. Characterization of an expanded glutamine repeat androgen receptor in a neuronal cell culture system. Neurobiol. Dis. 3, 313–323.
Dimos, J.T., et al., 2008. Induced pluripotent stem cells generated from patients with ALS can be differentiated into motor neurons. Science 321, 1218–1221.
Ebert, A.D., et al., 2009. Induced pluripotent stem cells from a spinal muscular atrophy patient. Nature 457, 277–280.
Egawa, N., et al., 2012. Drug screening for ALS using patient-specific induced pluripotent stem cells. Sci. Transl. Med. 4, 1–8.
Furutani, T., et al., 2002. Stabilization of androgen receptor protein is induced by agonist, not by antagonists. Biochem. Biophys. Res. Commun. 294, 779–784.
Hubbert, C., et al., 2002. HDAC6 is a microtubule-associated deacetylase. Nature 417, 455–458.
Iwata, A., et al., 2005. HDAC6 and microtubules are required for autophagic degradation of aggregated huntingtin. J. Biol. Chem. 280, 40282–40292.
Katsuno, M., et al., 2002. Testosterone reduction prevents phenotypic expression in a transgenic mouse model of spinal and bulbar muscular atrophy. Neuron 35, 843–854.
Katsuno, M., et al., 2006. Reversible disruption of dynactin 1-mediated retrograde axonal transport in polyglutamine-induced motor neuron degeneration. J. Neurosci. 26, 12106–12117.
Kawaguchi, Y., et al., 2003. The deacetylase HDAC6 regulates aggresome formation and cell viability in response to misfolded protein stress. Cell 115, 727–738.
Kennedy, W.R., et al., 1968. Progressive proximal spinal and bulbar muscular atrophy of late onset: a sex-linked recessive trait. Neurology 18, 671–680.
Kovacs, J.J., et al., 2005. HDAC6 regulates Hsp90 acetylation and chaperone-dependent activation of glucocorticoid receptor. Mol. Cell 18, 601–607.
La Spada, A.R., et al., 1991. Androgen receptor gene mutations in X-linked spinal and bulbar muscular atrophy. Nature 352, 77–79.
Montie, H.L., et al., 2011. SIRT1 modulates aggregation and toxicity through deacetylation of the androgen receptor in cell models of SBMA. J. Neurosci. 31, 17425–17436.
Nedelsky, N.B., et al., 2010. Native functions of the androgen receptor are essential to pathogenesis in a *Drosophila* model of spinobulbar muscular atrophy. Neuron 67, 936–952.
Nihei, Y., et al., 2013. Enhanced aggregation of androgen receptor in induced pluripotent stem cell-derived neurons from spinal and bulbar muscular atrophy. J. Biol. Chem. 288, 8043–8052.
Palazzolo, I., et al., 2009. Overexpression of IGF-1 in muscle attenuates disease in a mouse model of spinal and bulbar muscular atrophy. Neuron 63, 316–328.
Pandey, U.B., et al., 2007. HDAC6 rescues neurodegeneration and provides an essential link between autophagy and the UPS. Nature 447, 859–863.
Ranganathan, S., et al., 2009. Mitochondrial abnormalities in spinal and bulbar muscular atrophy. Hum. Mol. Genet. 18, 27–42.
Rhodes, L.E., et al., 2009. Clinical features of spinal and bulbar muscular atrophy. Brain 132, 3242–3251.
Schutz, S.V., et al., 2011. Inhibition of glycogen synthase kinase-3beta counteracts ligand-independent activity of the androgen receptor in castration resistant prostate cancer. PLoS ONE 6, e25341.
Sinclair, R., et al., 2007. Men with Kennedy disease have a reduced risk of androgenetic alopecia. Br. J. Dermatol. 157, 290–294.
Sommer, C.A., et al., 2009. Induced pluripotent stem cell generation using a single lentiviral stem cell cassette. Stem Cells 27, 543–549.
Subramandian, C., et al., 2011. HDAC6 deacetylates Ku70 and regulates Ku70-Bax binding in neuroblastoma. Neoplasia 13, 726–734.

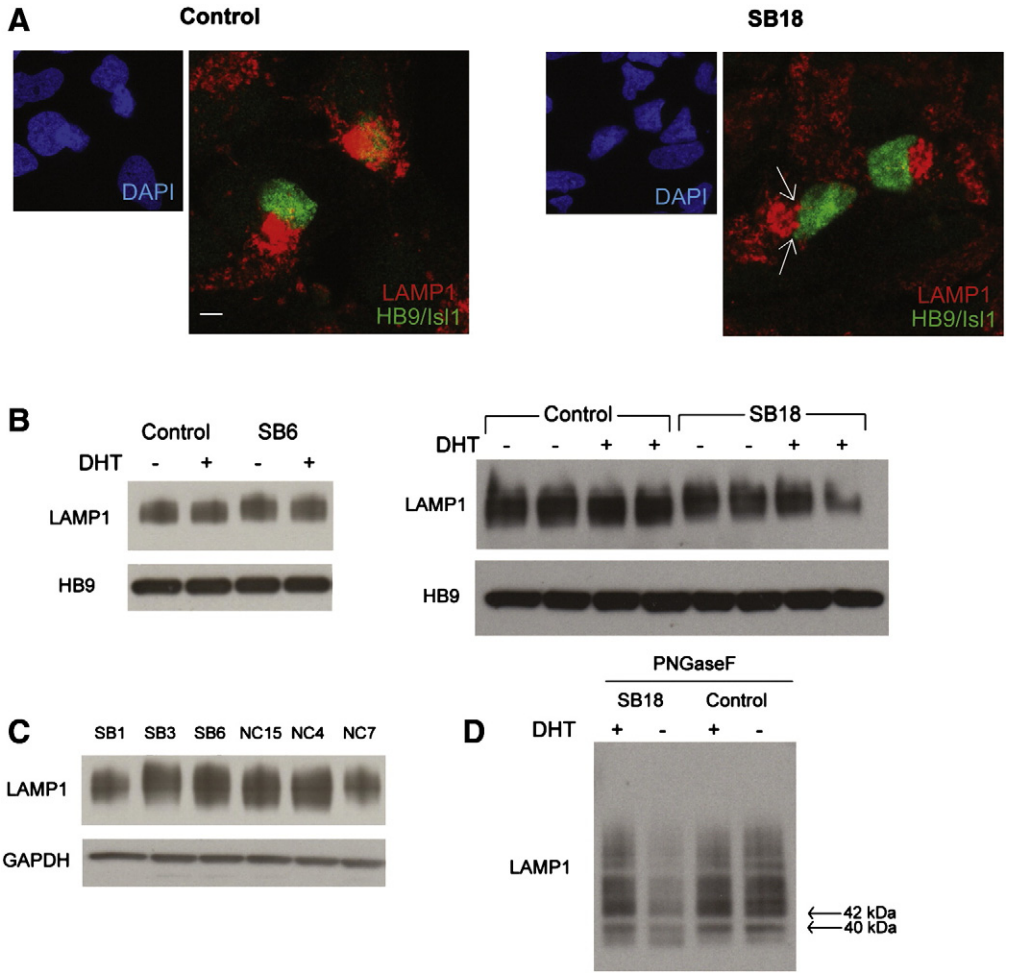

Fig. 6. Lysosomal staining and glycosylation in iPSC-derived motor neurons. (A) Immunofluorescent images showing loss of lysosome enrichment (arrows) around the microtubule organizing center in patient motor neurons (SB18) compared to control. Lysosomes are stained with LAMP1 (red) and HB9/Isl1 (green). Scale bar = 5 μm. (B) Western blot analysis of motor neuron extracts with and without DHT, showing increased molecular weight of LAMP1 in motor neuron extracts from two different patients (SB6 and SB18). (C) LAMP1 molecular weight shifts were not present in the undifferentiated iPSCs from three controls and three SBMA patients after 48 h of DHT treatment. (D) LAMP1 western blot analysis of control and patient (SB18) motor neurons after PNGase treatment showing equal molecular weights of the non-glycosylated LAMP1 proteins.

Tanaka, F., et al., 1999. Tissue-specific somatic mosaicism in spinal and bulbar muscular atrophy is dependent on CAG-repeat length and androgen receptor-gene expression level. Am. J. Hum. Genet. 65, 966–973.
Tapia, M., et al., 2010. Impaired function of HDAC6 slows down axonal growth and interferes with axonal initial segment development. PLoS ONE 5, e12908.
Vesa, J., et al., 2009. Valosin containing protein associated inclusion body myopathy: abnormal vacuolization, autophagy and cell fusion in myoblasts. Neuromuscul. Disord. 19, 766–772.
Xu, X., et al., 2011. Stage-specific germ-cell marker genes are expressed in all mouse pluripotent cell types and emerge early during induced pluripotency. PLoS ONE 6, e22413.
Zhang, L., et al., 1994. Studying human mutations by sperm typing: instability of CAG trinucleotide repeats in the human androgen receptor gene. Nat. Genet. 7, 531–535.
Zhang, X., et al., 2007. HDAC6 modulates cell motility by altering the acetylation level of cortactin. Mol. Cell 27, 197–213.